Dispersive analysis of $K_S \to \gamma\gamma$ and $K_S \to \gamma l^+ l^-$

2017 J. Phys.: Conf. Ser. 800 012034

(http://iopscience.iop.org/1742-6596/800/1/012034)

IOP Conf. Series: Journal of Physics: Conf. Series **800** (2017) 012034 doi:10.1088/1742-6596/800/1/012034

Dispersive analysis of $K_S \to \gamma\gamma$ and $K_S \to \gamma\ell^+\ell^-$

Lewis C. Tunstall,[0,1] **Gilberto Colangelo**[1] **and Ramon Stucki**[1]

[1]Albert Einstein Centre for Fundamental Physics, Institute for Theoretical Physics, University of Bern, Sidlerstrasse 5, CH–3012 Bern, Switzerland

E-mail: tunstall@itp.unibe.ch

Abstract. We calculate the decay rates for $K_S \to \gamma\gamma$ and $K_S \to \gamma\ell^+\ell^-$ ($\ell = e$ or μ) within a dispersive framework in which the weak Hamiltonian carries momentum. Given input from $K_S \to \pi\pi$ and $\gamma\gamma^{(*)} \to \pi\pi$, we solve the once-subtracted dispersion relations numerically and find that final-state $\pi\pi$ interactions generate sizeable corrections to the predictions from 3-flavour chiral perturbation theory. Our analysis predicts $\mathrm{BR}(K_S \to \gamma\gamma) = (2.34 \pm 0.31) \times 10^{-6}$, $\mathrm{BR}(K_S \to \gamma e^+ e^-) = (4.38 \pm 0.57) \times 10^{-8}$, and $\mathrm{BR}(K_S \to \gamma\mu^+\mu^-) = (1.45 \pm 0.27) \times 10^{-9}$.

1. Motivation

The advent of high-statistics kaon experiments such as NA62 [1], KLOE-2 [2] and (somewhat surprisingly) LHCb [3], presents an opportunity for theorists to re-examine the Standard Model (SM) background for various rare decays. In order to identify areas where progress may be made, it is useful to adopt a classification system of the possible decay modes:

- ☺ **The good:** so-called golden modes like $K \to \pi\nu\bar{\nu}$, where the dominant effect is of short-distance nature and the corresponding hadronic matrix element is largely determined by a single form factor;[1]
- 😐 **The bad:** CP-violating decays like $K_L \to \pi^0\ell^+\ell^-$ ($\ell = e$ or μ), where short- and long-distance effects come in roughly equal measure;
- ☹ **The ugly:** non-leptonic decays like $K_S \to \pi\pi$ and $K_L \to 3\pi$ which are dominated by long-distance contributions. In such cases, non-perturbative methods are essential; especially to make sense of long-standing puzzles like the $\Delta I = 1/2$ rule (which for the purposes of this talk is assumed to be exact).

In between the above trio are decays where a separation of the short- and long-distance effects can be achieved with varying degree of success. Since kaon decays occur at low energies, a systematic analysis can be undertaken within $\chi\mathrm{PT}_3$, where amplitudes are expanded as an asymptotic series in powers of $O(m_K)$ momentum and light quark masses $m_{u,d,s} = O(m_K^2)$. In general, our ability to obtain precise predictions from the effective field theory is influenced by two main factors:

(i) hadronic uncertainties are parametrised in terms of low-energy constants (LECs) like the pion decay constant F_π, whose values are not fixed by chiral symmetry alone. In an ideal

[0] Speaker

[1] However, as remarked at this conference [4], "good" does not necessarily imply "trivial": e.g. for $K \to \pi\nu\bar{\nu}$ there are also bi-local, long-distance contributions, whose evaluation requires input from lattice QCD.

world, these LECs would be extracted from a combination of input from experiment and lattice QCD. However, for the weak radiative decays which interest us, this reality appears to be far into the future;

(ii) at energies above the $\pi\pi$ threshold, final-state interactions (FSI), especially in the 0^{++} channel [5–8], can spoil the convergence of the χPT_3 expansion. In these cases, chiral-perturbative methods must be abandoned in favour of non-perturbative methods based on unitarity, analyticity, and crossing symmetry.

Dispersion relations offer a means to address items (i) and (ii) within a model-independent framework. In this talk we consider the application of these methods to $K_S \to \gamma\gamma^*$ transitions [11], with the two-fold aim of (a) extending the predictions from LO χPT_3 to fully account for effects due to FSI, and (b) providing a reliable estimate for the theory uncertainty. For the pure radiative decay, the chiral prediction [12–14] for the rate

$$\text{BR}(K_S \to \gamma\gamma)_{\chi\text{PT}_3} = 2.0 \times 10^{-6} \tag{1}$$

is in reasonable agreement with the experimental average

$$\text{BR}(K_S \to \gamma\gamma) = (2.63 \pm 0.17) \times 10^{-6}\,, \tag{2}$$

while the predictions [15] for the leptonic modes are typically expressed in terms of the ratios

$$\left.\frac{\Gamma(K_S \to \gamma\ell^+\ell^-)}{\Gamma(K_S \to \gamma\gamma)}\right|_{\chi\text{PT}_3} = \begin{cases} 1.6 \times 10^{-2} & (\ell = e) \\ 3.8 \times 10^{-4} & (\ell = \mu) \end{cases}\,. \tag{3}$$

Although these decays have not yet been measured, they may lie within reach of LHCb's kaon programme or the KLOE-2 experiment, which is projected to be sensitive down to K_S branching ratios of $O(10^{-9})$. As shown below, the dispersive analysis yields sizeable corrections to the predictions from LO χPT_3. Our results support the generally accepted view that getting FSI under good control is essential if long-distance contributions to 0^{++} channels are to be reliably determined.[2]

2. Dispersive framework for $K_S \to \gamma\gamma^*$

In two-body decays, the kinematics is completely fixed and thus a representation of the amplitude in terms of Mandelstam variables s, t, u is not immediately forthcoming. One popular approach is to promote the mass of the decaying particle to a dynamical variable "s" and solve the corresponding dispersion integral. Although seductively simple, this prescription is subject to an inherent ambiguity associated with the fact that there are an *infinite number of ways* in which to extrapolate the mass off-shell [19, 20].

In order to avoid the arbitrariness induced by off-shell extrapolations, an alternative approach was proposed by Büchler *et al.* [21] in the study of $K_S \to \pi\pi$. The key idea in that work was to allow the $\Delta S = 1$ weak Hamiltonian $\mathcal{H}_w$ to inject momentum in the amplitude $\langle\pi\pi|\mathcal{H}_w|K_S\rangle$, and solve the resulting set of coupled dispersion integrals in the crossed s, t, u channels. Adapted to $K_S \to \gamma\gamma^*$ transitions (Fig. 1), this prescription yields a tensor decomposition of the amplitude[3]

$$A_{\mu\nu}(k, q_1, q_2) \supset \big(q_1 \cdot q_2 g_{\mu\nu} - q_{2\mu} q_{1\nu}\big) A_{\gamma\gamma^*}(s, t, u, q_2^2) \tag{4}$$

[2] A topical example concerns the SM prediction for ϵ'/ϵ, where the recent lattice result from RBC/UKQCD [16] is in tension with experiment at approximately the 3σ confidence level. However, that same calculation produces a $\pi\pi$ scattering phase-shift $\delta_0^0(m_K^2)$ that falls $\approx 3\sigma$ short of model-independent analyses based on the Roy equations. This suggests that the effects from FSI are not (yet) fully accounted for in the lattice result; see e.g. [17, 18] for further details.

[3] The most general tensor decomposition actually involves three scalar functions, but two of them vanish if contributions from D waves and higher are neglected; see main text.

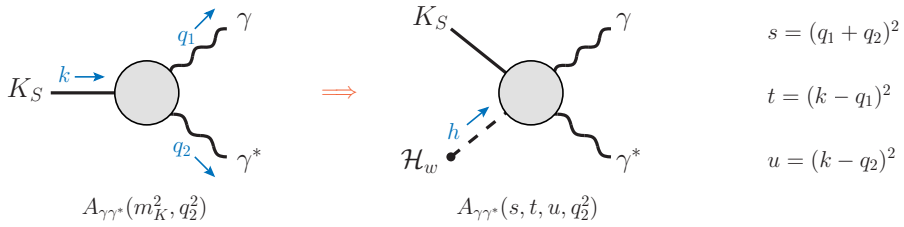

Figure 1. For the physical decay amplitude $A_{\gamma\gamma^*}$ (left), the kinematics are completely fixed by the external momenta. Allowing the weak Hamiltonian $\mathcal{H}_w$ to carry momentum (right) promotes $A_{\gamma\gamma^*}$ to a function of s, t, u, with the physical amplitude recovered by taking the limit $h \to 0$.

that involves a scalar function $A_{\gamma\gamma^*}$ which depends on s, t, u and is free from kinematic zeros and singularities. A straightforward one-loop calculation determines the LO χPT$_3$ result for $A_{\gamma\gamma^*}$ in this framework, and reproduces the predictions listed in eqs. (1) and (3) once the physical limit $h \to 0$ is taken.

Our goal, however, is to construct a dispersive representation for $A_{\gamma\gamma^*}$, which in general requires an analysis of all possible intermediate states $\pi\pi$, 4π, KK, ... in all three channels. This is rather complicated, so instead we make use of a simplification which has proven to be particularly effective for other scattering processes at low energies, namely to neglect the contributions to discontinuities coming from D waves and higher. As in those cases, we expect that at the physical point $h \to 0$, the contributions to the S wave coming from discontinuities in the t and u channels are negligible.

In the s-channel, the leading contribution to the discontinuity of $A_{\gamma\gamma^*}$ is due to the $\pi\pi$ intermediate state. The unitarity relation for this contribution reads

$$\mathrm{disc}_s\, A_{\gamma\gamma^*}(s, q_2^2) = -\alpha\sqrt{1-4m_\pi^2/s}\left\{\frac{A_{\pi\pi}(s)[h^0_{++}(s,q_2^2)]^*}{2(s-q_2^2)}\right\}, \tag{5}$$

so we write down a once-subtracted dispersion relation

$$A_{\gamma\gamma^*}(s, s_0, q_2^2) = a_{\gamma\gamma^*}(s_0, q_2^2) + \frac{s-s_0}{\pi}\int_{4m_\pi^2}^{\infty} dz\, \frac{\mathrm{disc}_s\, A_{\gamma\gamma^*}(z, q_2^2)}{(z-s_0)(z-s-i\epsilon)}\,, \tag{6}$$

where the subtraction constant $a_{\gamma\gamma^*}$ is needed to ensure convergence of the integral. Evidently, knowledge of $a_{\gamma\gamma^*}$ and the discontinuity (5) completely fixes the prediction for $A_{\gamma\gamma^*}$. Concerning quantities which enter in the latter, h^0_{++} is a helicity partial wave corresponding to the $\gamma\gamma^* \to \pi\pi$ subprocess, while $A_{\pi\pi}$ is the $K_S \to \pi\pi$ amplitude, whose dispersive representation [21] given to good approximation by

$$A_{\pi\pi}(s) \simeq \sqrt{2}a_{\pi\pi}[1 + E(X)s/m_K^2]\Omega_0^0(s)\,. \tag{7}$$

Here $a_{\pi\pi}$ is a subtraction constant whose value is fixed from the physical $K_S \to \pi\pi$ decay amplitude at $s = m_K^2$, while the quantity

$$E(X) = \frac{3m_K^2(1+X)}{m_K^2 - m_\pi^2(4+3X)} \tag{8}$$

parametrises the NLO corrections in terms of the parameter X. An appealing feature of this representation is that the effects from FSI are fully accounted for in terms of the calculable Omnès factor

$$\Omega_0^0(s) = \exp\left(\frac{s}{\pi}\int_{4m_\pi^2}^{\infty} dz\, \frac{\delta_0^0(z)}{z(z-s-i\epsilon)}\right). \tag{9}$$

3. Dispersive treatment of $K_S \to \gamma\gamma$

With a dispersive representation of the $K_S \to \gamma\gamma^*$ amplitude at hand (6), our first application concerns the case where both photons are on-shell. Here, the subtraction constant $a_{\gamma\gamma}$ is fixed by matching to χPT$_3$ well below the $\pi\pi$ threshold, where the typically large corrections due to FSI are entirely absent. In particular, we match at the kinematic point $s_0 = -0.098$ GeV^2, where the χPT$_3$ amplitude vanishes and thus the dependence on $a_{\gamma\gamma}$ is eliminated — up to $O(p^6)$ corrections which we fold into our final estimate of the systematic uncertainty.

Regarding the input for $h^0_{0,++}$, we use data from the coupled-channel analysis of $\gamma\gamma \to \pi\pi$ performed by García-Martín and Moussallam [22]. Since the determination of $h^0_{0,++}$ in this analysis is expected to be reliable up to $s \lesssim 2$ GeV^2, it is necessary to impose a cutoff Λ in our dispersion integral. We have checked that at the physical point $s = m_K^2$, the cutoff dependence is very mild, and we take $\Lambda = 1.2$ GeV as a benchmark value.

The resulting energy dependence of the real and imaginary parts of $A_{\gamma\gamma}$ is shown in Fig. 2. As expected, the dispersive representation agrees with LO χPT$_3$ below the $\pi\pi$ threshold, but for $s > 4m_\pi^2$, the effects from FSI distort the amplitude, producing a significant enhancement (suppression) of the real (imaginary) part. These effects lead to an enhanced prediction for the branching ratio

$$\mathrm{BR}(K_S \to \gamma\gamma) = \frac{m_K^3}{64\pi}\frac{|A_{\gamma\gamma}(m_K^2)|^2}{\Gamma(K_S)_{\mathrm{tot}}} = (2.34 \pm 0.31) \times 10^{-6} \tag{10}$$

which brings the SM and experiment (2) into much better agreement. The quoted uncertainty is due to four main sources of systematic error which enter in our analysis:

- the variation $X = \pm 0.3$ based on the expected convergence pattern of χPT$_3$ below the $\pi\pi$ threshold;
- $O(p^6)$ corrections to the subtraction constant $a_{\gamma\gamma}$, which we estimate by shifting the value of the subtraction point s_0 by 30%;
- lack of knowledge about the phase of the $K_S \to \pi\pi$ sub-amplitude in the inelastic region. We account for this by comparing two Omnès factors which exhibit "dip" and "non-dip" behaviour in this kinematic region;
- contributions from the high-energy region $\Lambda > 1.2$ GeV. These we estimate by guiding the phase of Ω_0^0 to π and fixing the helicity partial wave to a constant value $|h_{0,++}| \approx 4$.

Combined in quadrature, the final uncertainty has turned out to be remarkably modest.

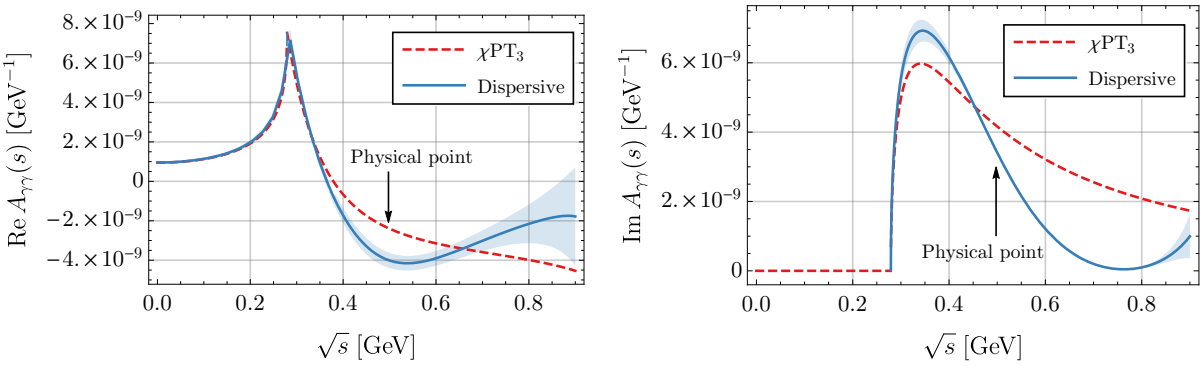

Figure 2. Energy dependence of the real (left) and imaginary (right) parts of the $K_S \to \gamma\gamma$ amplitude. The blue band in the dispersive result corresponds to the systematic uncertainty.

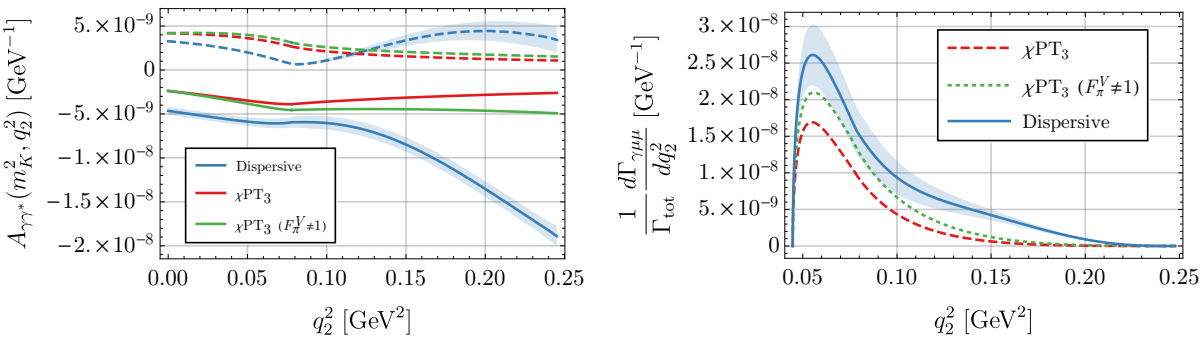

Figure 3. Dependence of the $K_S \to \gamma\gamma^*$ amplitude (left) and $K_S \to \gamma\mu^+\mu^-$ differential decay rate (right) on the photon momentum q_2^2. In the left figure, the real parts are denoted by the solid curves, while the imaginary parts are dashed. The bands on the dispersive results correspond to the systematic uncertainty.

4. Dispersive treatment of $K_S \to \gamma\ell^+\ell^-$

We now consider the $K_S \to \gamma\gamma^*$ transition, where the photon momentum lies in the physical region $4m_\ell^2 \le q_2^2 \le m_K^2$ relevant for $K_S \to \gamma\ell^+\ell^-$ decays. In this case, we subtract the dispersion integral (6) at $s_0 = 0$, and fix the subtraction constant $a_{\gamma\gamma^*}$ by matching to the χPT$_3$ amplitude. Regarding input for the discontinuity, we use the pion form factor and helicity partial wave $h_{0,++}$ obtained from Moussallam's single-channel analysis of $\gamma\gamma^* \to \pi\pi$ [23]. Strictly speaking, the input for $h_{0,++}$ is only valid for energies $\sqrt{s} \lesssim 0.8$ GeV, however, we have checked that increasing the cutoff to $\Lambda = 1.2$ GeV does not lead to a difference of more than $\approx 7\%$ in the resulting prediction for $A_{\gamma\gamma^*}$. Since this small change is covered by our estimate of the systematic uncertainty, we take the larger cutoff as a benchmark value in our numerics

For fixed $s = m_K^2$, we evaluate the dispersion integral numerically and show the q_2^2 dependence of the amplitude in the left plot of Fig. 3. As shown in the figure, when $q_2^2 < 4m_\pi^2$, the effect of FSI resembles that seen in $K_S \to \gamma\gamma$ (Fig. 2), with the real (imaginary) parts enhanced (suppressed) relative to χPT$_3$. However, as q_2^2 increases above the $\pi\pi$ threshold, the pion vector form factor F_π^V becomes progressively more important, and both real and imaginary parts in the dispersive amplitude are enhanced relative to LO χPT$_3$.

Turning to the $K_S \to \gamma\ell^+\ell^-$ decay rates, in Fig. 3 we compare the χPT$_3$ prediction for the differential decay rate involving muons against our dispersive result. Evidently, the corrections are large for $q_2^2 \gtrsim 0.05$: this can be inferred from the q_2^2 behaviour shown in the left plot in Fig. 3. We also see that, for this mode, the dominant source of the enhancement is due to the pion form factor.

The resulting branching fractions are given in Table 1, where the uncertainties are determined as in Sec. 2, except for the subtraction constant: here we keep s_0 fixed and vary the χPT$_3$ amplitude by 30%. In both cases, the corrections are sizeable: for the electron mode we see a shift of $O(50\%)$, while in the muon mode we have a shift of $O(100\%)$. The origin of these shifts are different in each case. For the electron mode, the phase space is peaked near the origin $q_2^2 = 0$, so the role of F_π^V is suppressed and the dominant effect is due to FSI. On the other hand, as shown in the right plot of Fig. 3, the enhancement in the muon mode is due to both FSI and the form factor.

Input	$\mathrm{BR}(K_S \to \gamma e^+ e^-)$	$\mathrm{BR}(K_S \to \gamma \mu^+ \mu^-)$
$\chi\mathrm{PT}_3$	3.09×10^{-8}	7.25×10^{-10}
$\chi\mathrm{PT}_3$ ($F_\pi^V \neq 1$)	3.17×10^{-8}	9.97×10^{-10}
This work	$(4.38 \pm 0.57) \times 10^{-8}$	$(1.45 \pm 0.27) \times 10^{-9}$

Table 1. Predictions for the branching ratio of $K_S \to \gamma\ell^+\ell^-$. The second row indicates the effect of including the pion vector form factor F_π^V in the $\chi\mathrm{PT}_3$ amplitude.

5. Remarks

Chiral perturbation theory and lattice QCD are two of the main tools which allow a systematic calculation of long-distance contributions to kaon decays, but getting FSI under good control in either of these approaches is challenging. Dispersion relations offer a different, complementary methodology to the previous two, which addresses specifically the treatment of FSI. If one can match the dispersive and the chiral representation, and solve the dispersion relation, one can usually obtain much better control over FSI effects. In this talk, we have presented a first step in this direction by introducing a dispersive framework for $K_S \to \gamma\gamma$ and $K_S \to \gamma\ell^+\ell^-$. In both cases we find the corrections due to FSI are large with respect to LO $\chi\mathrm{PT}_3$. The extension of this framework to the more challenging $K_S \to \ell^+\ell^-$ decays is currently in progress.

Acknowledgements

LCT thanks the conference organisers for the opportunity to present the work discussed in this article. We also thank Marc Knecht and Peter Stoffer for helpful discussions regarding the systematic uncertainties in our analysis. Financial support from the Swiss National Science Foundation is gratefully acknowledged.

References

[1] G. Collazuol [NA62 Collaboration], PoS EPS **-HEP2009** (2009) 260.
[2] G. Amelino-Camelia *et al.*, Eur. Phys. J. C **68** (2010) 619 [arXiv:1003.3868].
[3] R. Aaij *et al.* [LHCb Collaboration], JHEP **1301**, 090 (2013) [arXiv:1209.4029].
[4] G. Isidori, these proceedings [URL: http://tinyurl.com/kaonsummary].
[5] A. Neveu and J. Scherk, Annals Phys. **57** (1970) 39.
[6] T. N. Truong, Acta Phys. Polon. B **15** (1984) 633.
[7] T. N. Truong, Phys. Lett. B **207** (1988) 495.
[8] A. Dobado, M. J. Herrero and T. N. Truong, Phys. Lett. B **235** (1990) 134.
[9] J. R. Pelaez, Phys. Rept. **658**, 1 (2016) [arXiv:1510.00653].
[10] I. Caprini, G. Colangelo and H. Leutwyler, Phys. Rev. Lett. **96** (2006) 132001 [arXiv:hep-ph/0512364].
[11] G. Colangelo, R. Stucki and L. C. Tunstall, Eur. Phys. J. C (to be published) [arXiv:1609.03574].
[12] G. D'Ambrosio and D. Espriu, Phys. Lett. B **175** (1986) 237.
[13] J. L. Goity, Z. Phys. C **34** (1987) 341.
[14] V. Cirigliano, G. Ecker, H. Neufeld, A. Pich and J. Portoles, Rev. Mod. Phys. **84** (2012) 399 [arXiv:1107.6001].
[15] G. Ecker, A. Pich and E. de Rafael, Nucl. Phys. B **303** (1988) 665.
[16] Z. Bai *et al.* [RBC and UKQCD Collaborations], Phys. Rev. Lett. **115**, 212001 (2015) [arXiv:1505.07863].
[17] G. Colangelo, talk at NA62 Kaon Physics Handbook MITP Workshop, 11-22 January, 2016 [URL: http://tinyurl.com/NA62colangelo].
[18] A. Pich, talk at NA62 Kaon Physics Handbook MITP Workshop 11-22 January, 2016 [URL: http://tinyurl.com/NA62pich].
[19] G. Colangelo, Nucl. Phys. Proc. Suppl. **106** (2002) 53 [arXiv:hep-lat/0111003].
[20] M. Büchler, G. Colangelo, J. Kambor and F. Orellana, Phys. Lett. B **521** (2001) 29 [arXiv:hep-ph/0102289].
[21] M. Büchler, G. Colangelo, J. Kambor and F. Orellana, Phys. Lett. B **521** (2001) 22 [arXiv:hep-ph/0102287].
[22] R. García-Martín and B. Moussallam, Eur. Phys. J. C **70** (2010) 155 [arXiv:1006.5373].
[23] B. Moussallam, Eur. Phys. J. C **73** (2013) 2539 [arXiv:1305.3143].